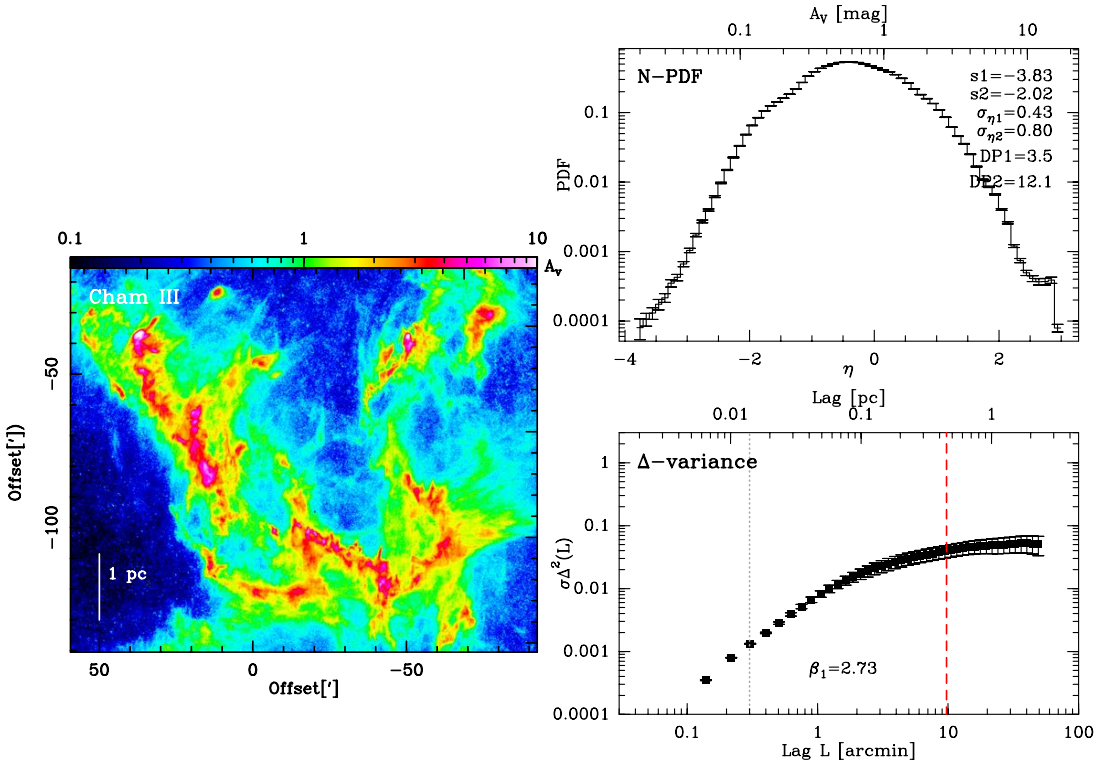

Fig. C.26: Chamaeleon III: Fig. caption see Fig. C.1.

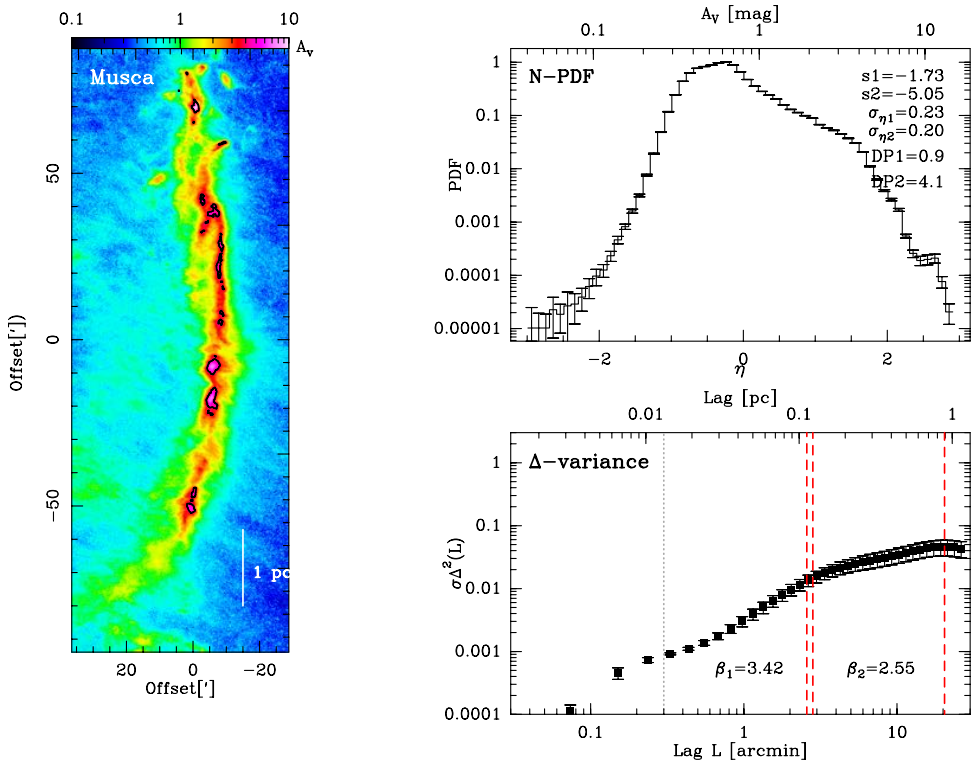

Fig. C.27: MUSCA: Fig. caption see Fig. C.1.

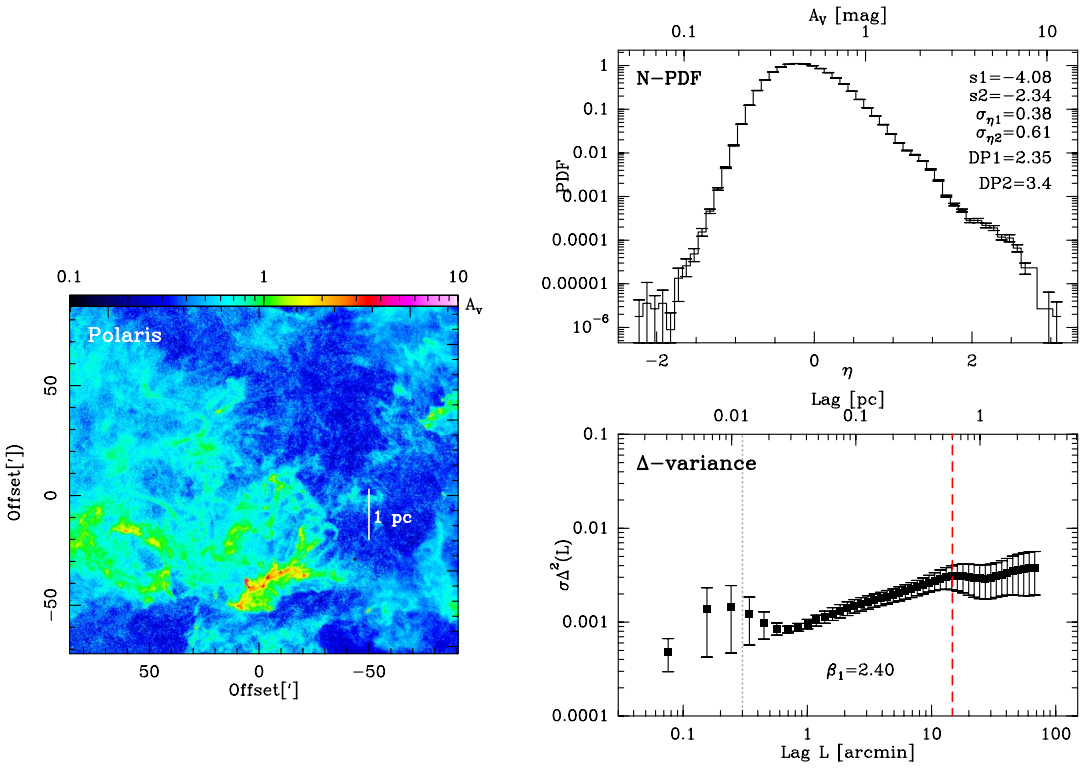

Fig. C.28: POLARIS: Fig. caption see Fig. C.1.

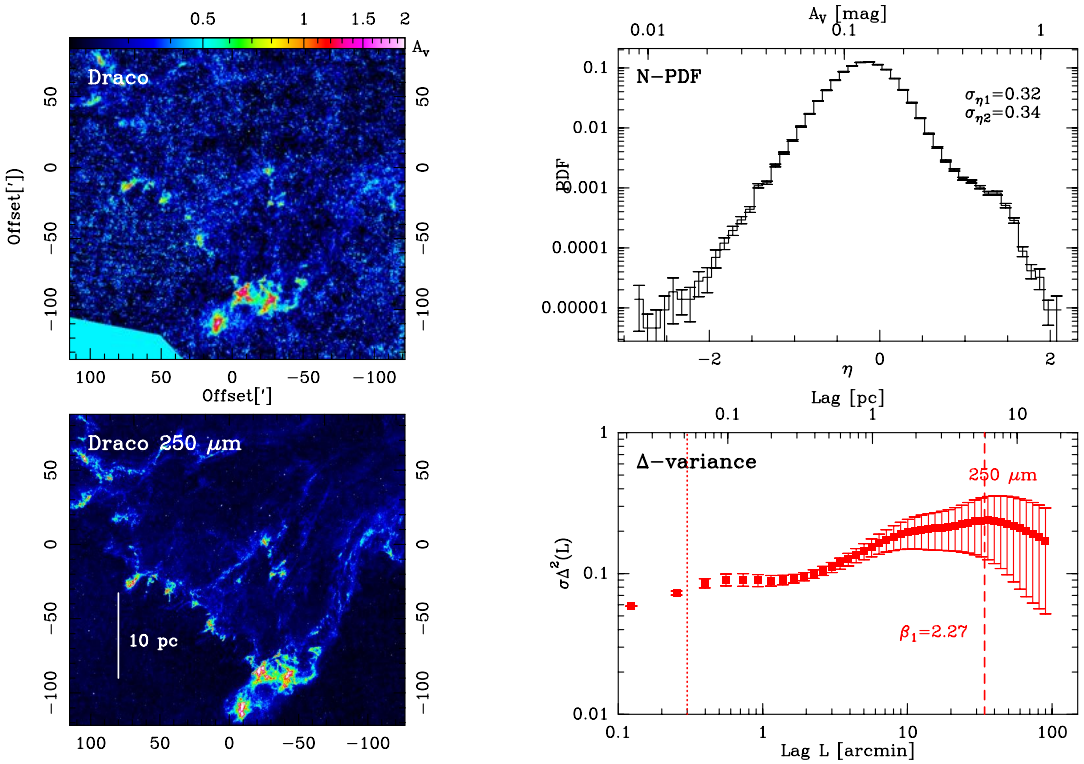

Fig. C.29: DRACO: Fig. caption see Fig. C.1.

Appendix D: Individual N-PDFs

Figures D.1 to D.29 display the N-PDFs of all clouds and the best fitting model. For all regions where we applied a LOS correction, we used this column density for performing the N-PDF. The models are indicated in the figure caption and follow the syntax explained in Sec. 2.4.1, (1) ELP: a single log-normal (L) convolved with a Gaussian noise distribution that creates an error slope (E) on the left-hand side and a power law tail (P); (2) ELLP: the same as (1) but with two log-normals, (3) LL2P: Two log-normals and two PLTs, (4) EL2P: the same as (1) but with two PLTs, (5) ELL2P: the same as (2) but with 2 PLTs.

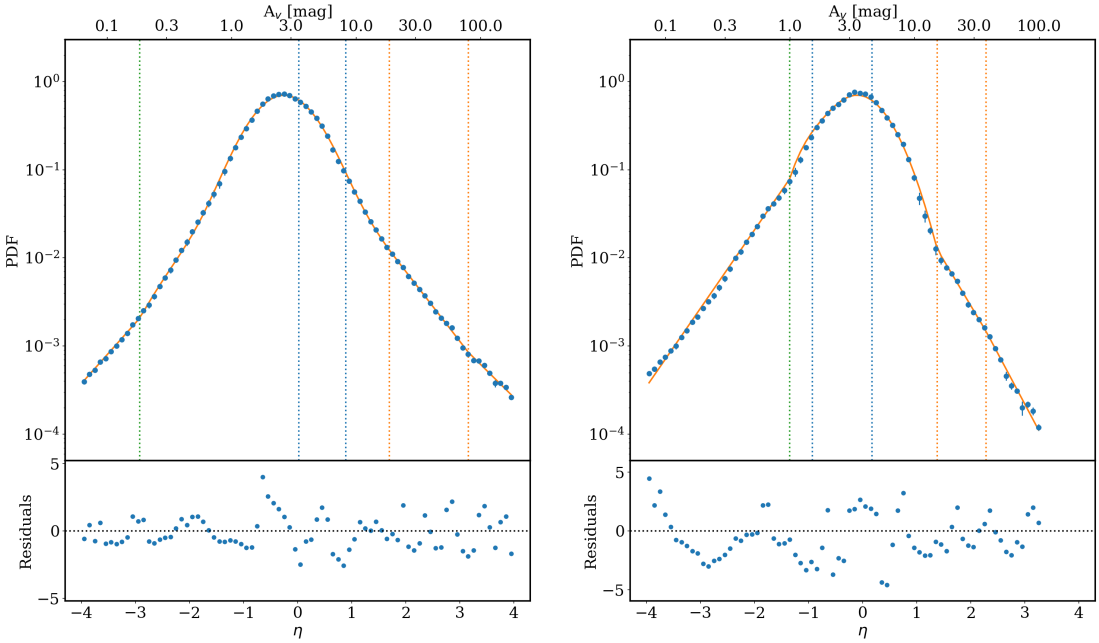

Fig. D.1: N-PDFs of LOS corrected column density (blue points), expressed in visual extinction (upper x-axis) and in η (lower x-axis) of DR21 (left) and DR15 (right). The left y-axis gives the PDF (there can be small differences compared to the plots in Appendix C because for the model fit, we excluded the extreme low- and high density ranges, which leads to a slightly different normalization). The orange curve indicates the best fitting model for the N-PDF (see Table B.1 and B.2). The vertical lines show the peak values of the log-normal(s) in blue, the break points for the power laws in orange and the error power law break point in green. Underneath is the standardized residuals, a perfect model would give numbers with mean of 0 and a variance of 1.

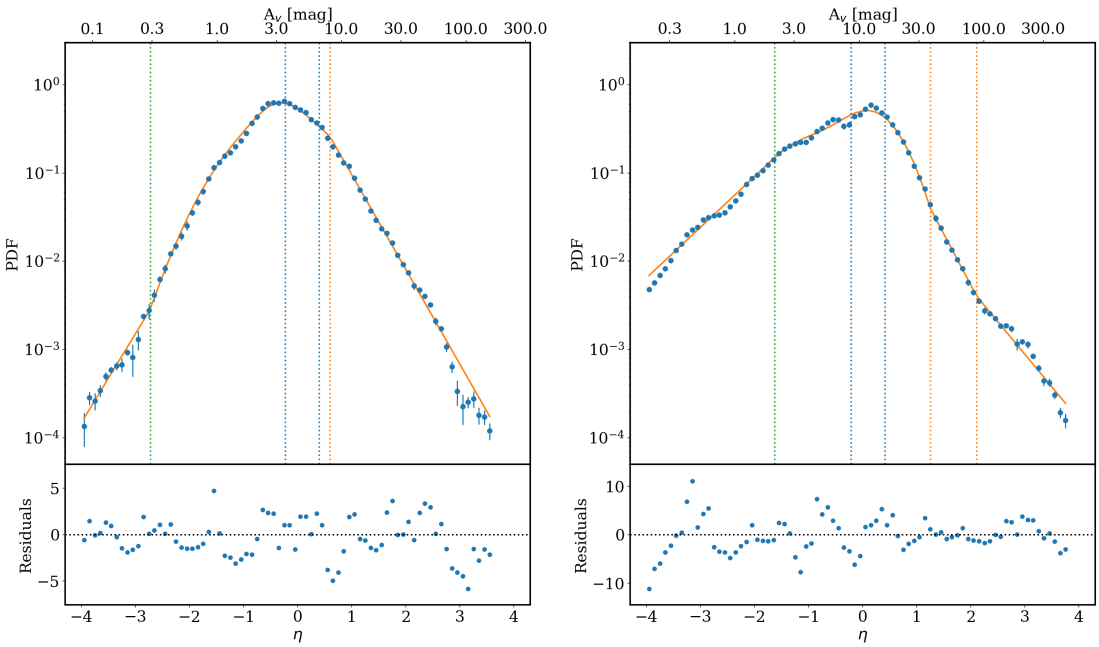

Fig. D.2: M16 (left) and M17 (right).

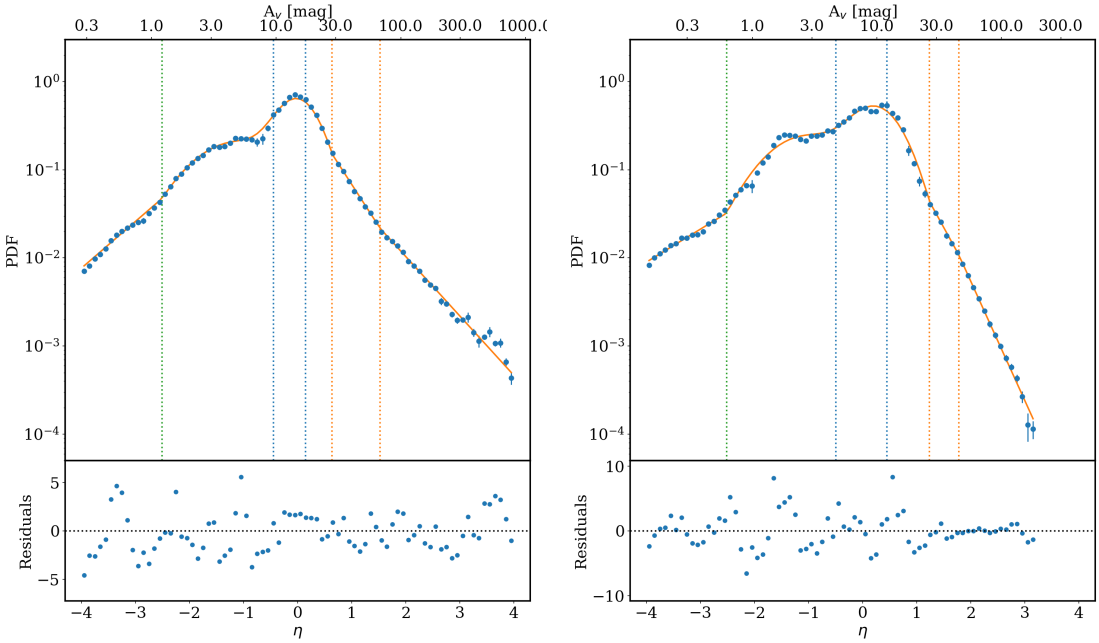

Fig. D.3: NGC6334 (left) and NGC6357 (right).

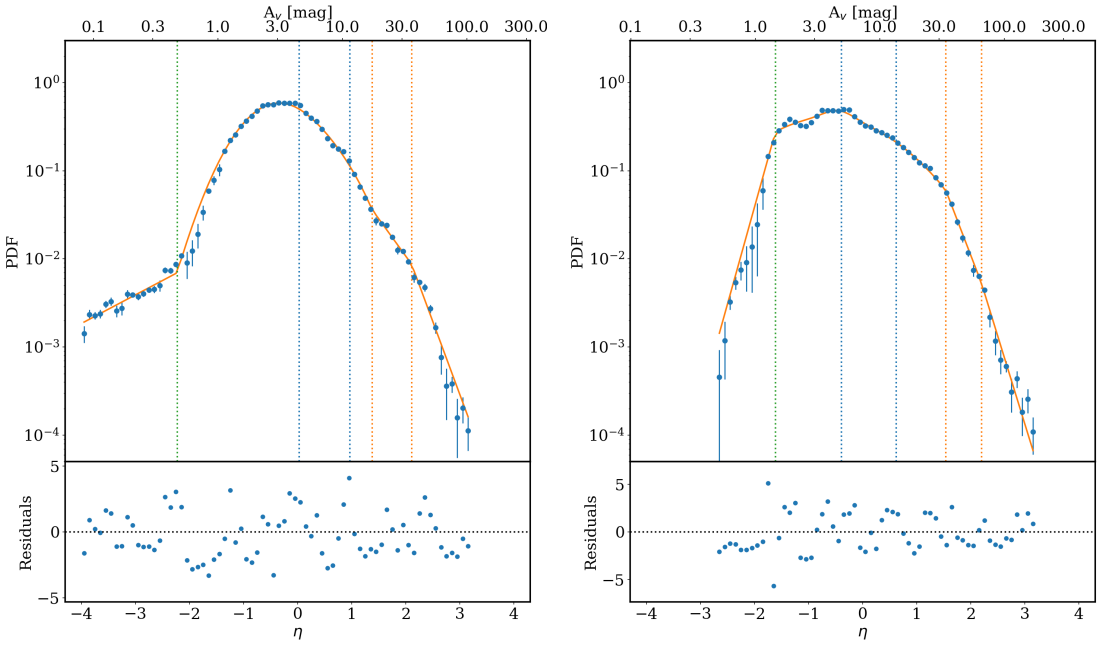

Fig. D.4: Rosette (left) and Vela (right).

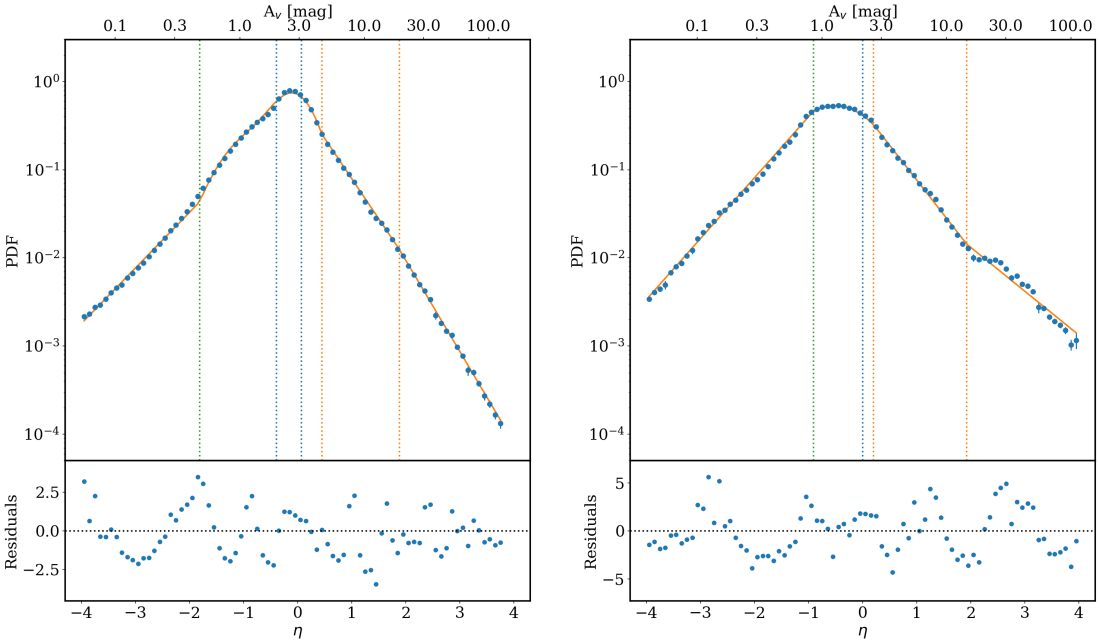

Fig. D.5: Aquila (left) and Mon R2 (right).

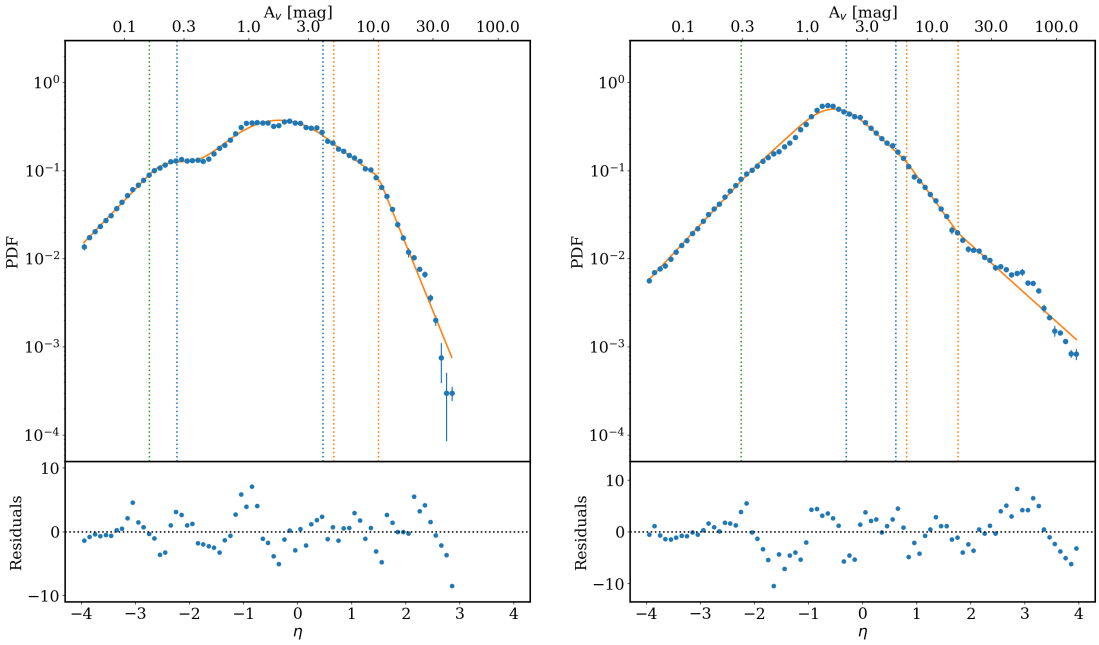

Fig. D.6: MonOB1 (left) and NGC2264 (right).

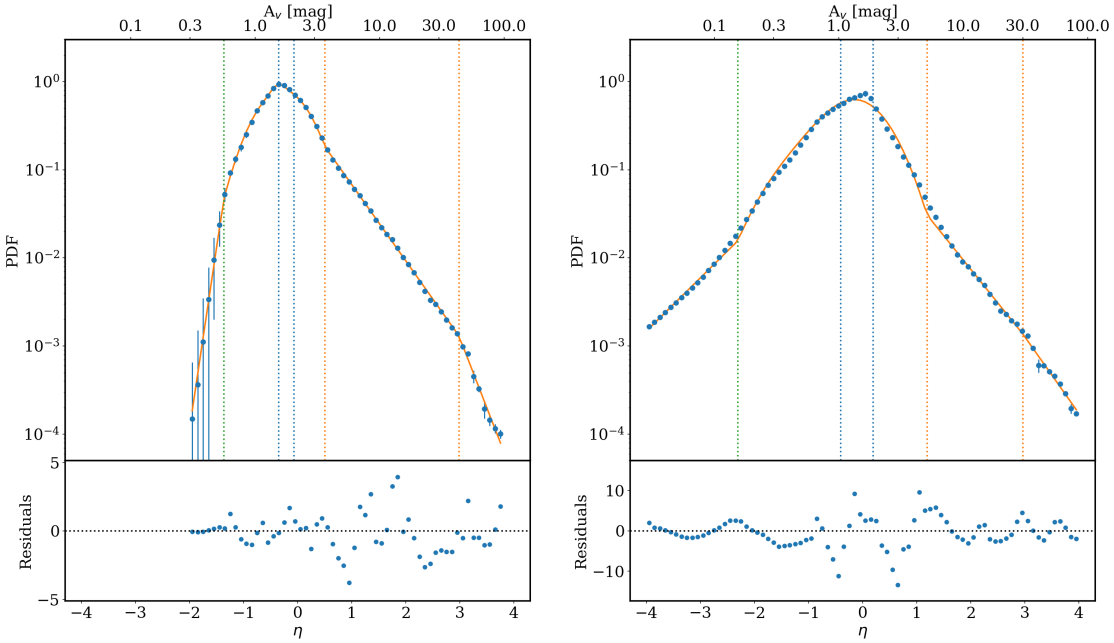

Fig. D.7: Orion B (left) and Serpens (right).

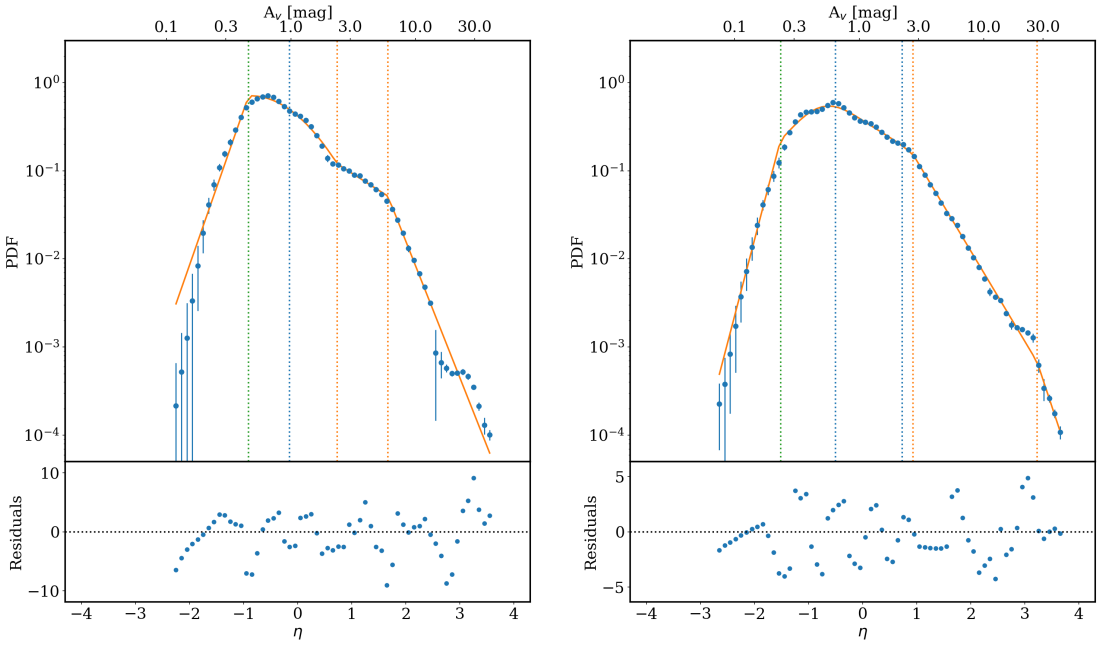

Fig. D.8: ChamI (left) and ChamII (right).

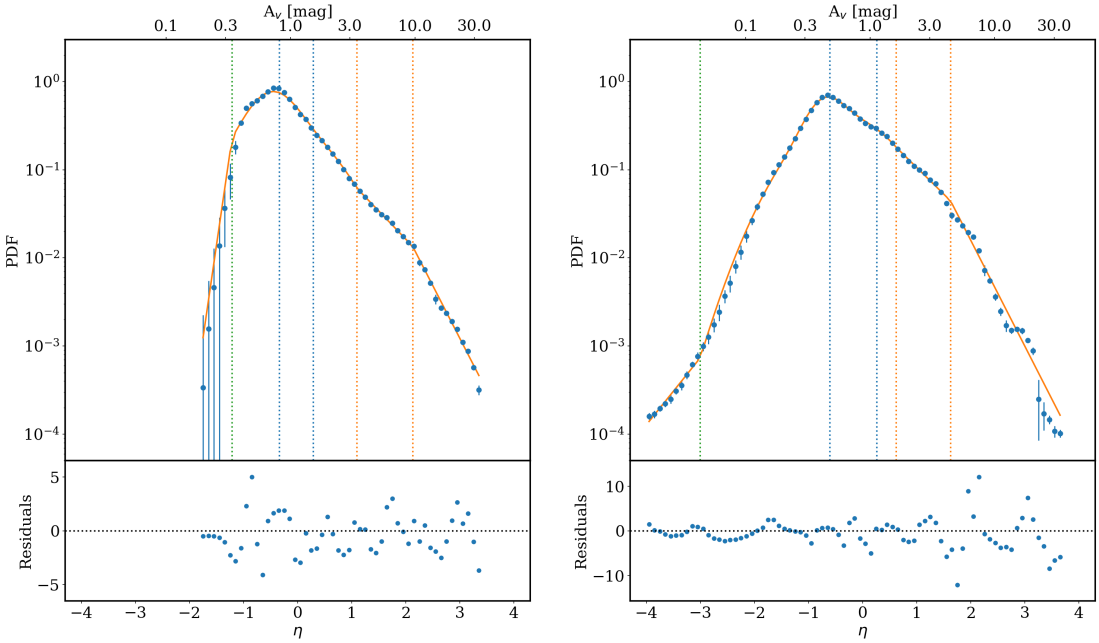

Fig. D.9: IC5146 (left) and Lupus I (right).

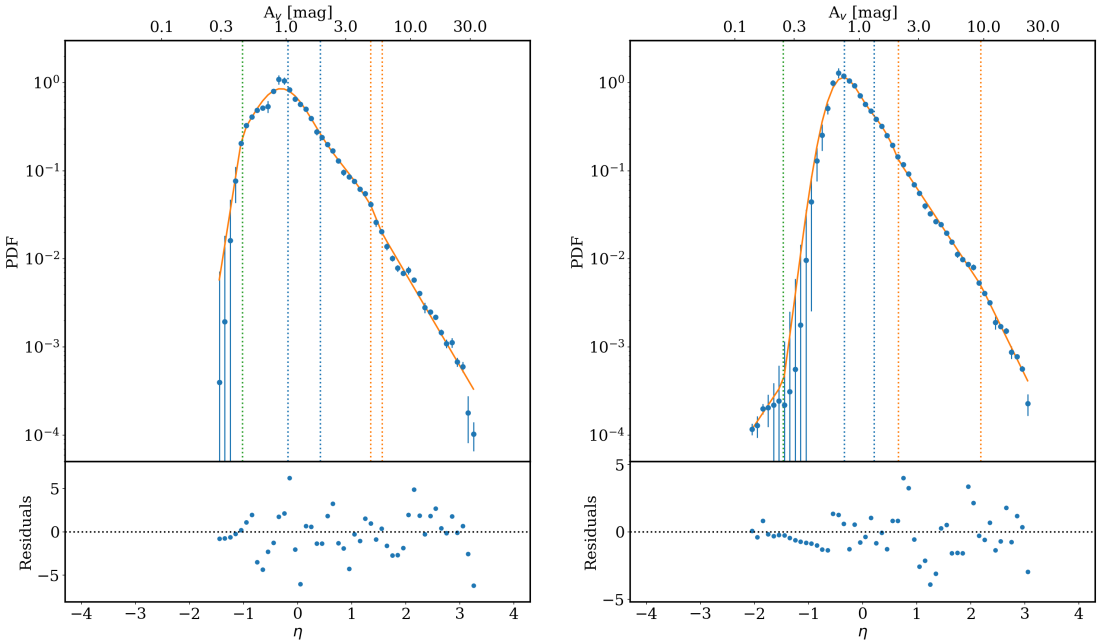

Fig. D.10: Lupus III (left) and Lupus IV (right).

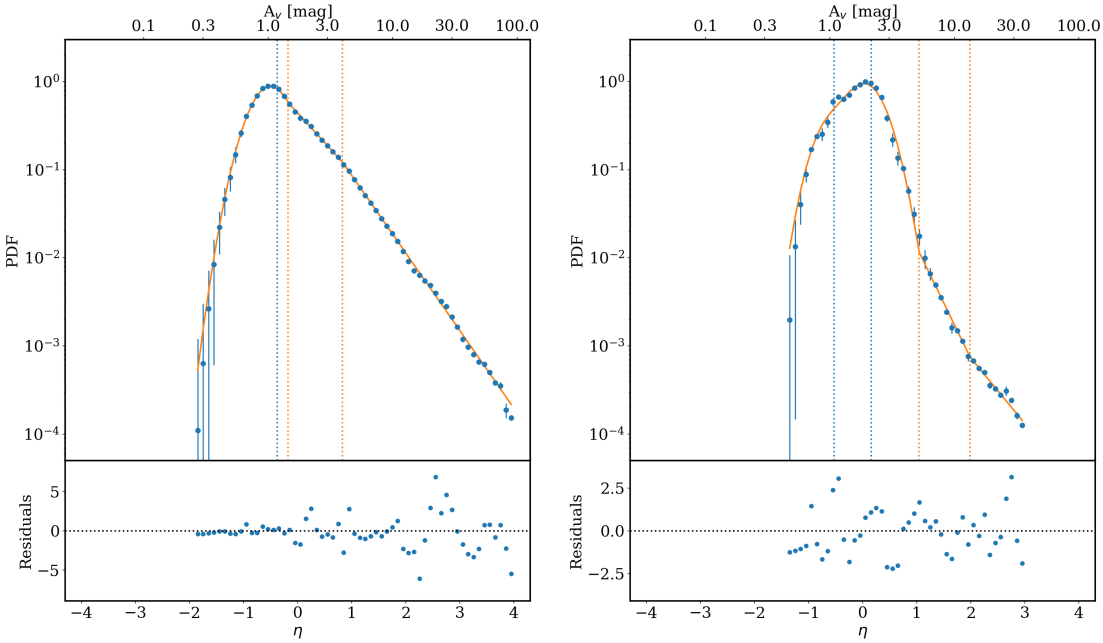

Fig. D.11: Perseus (left) and Pipe (right).

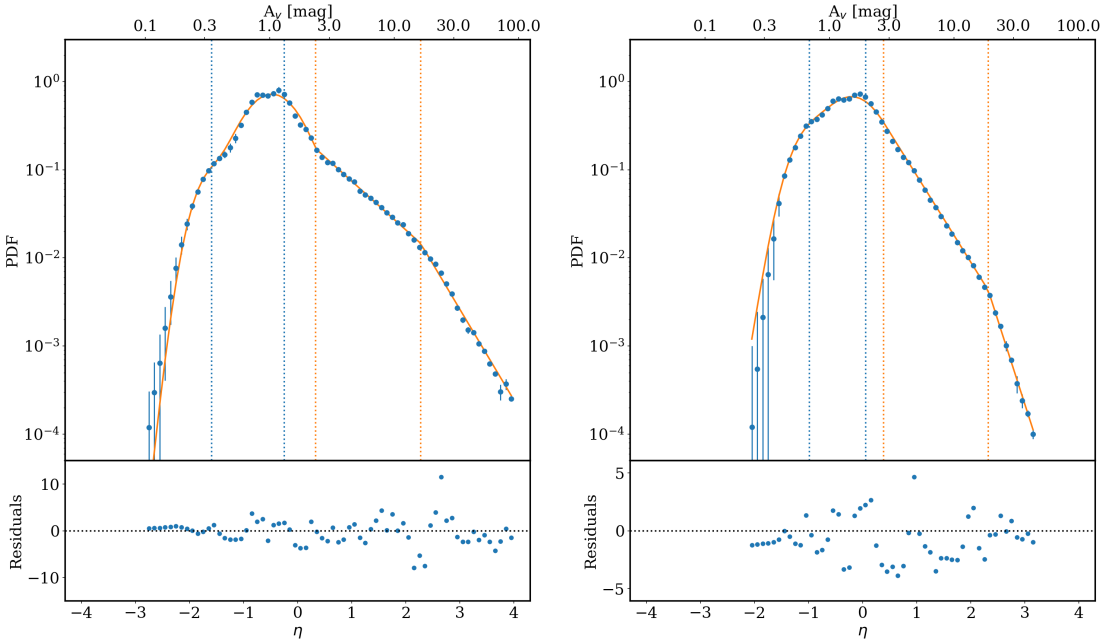

Fig. D.12: Rhooph (left) and Taurus (right).

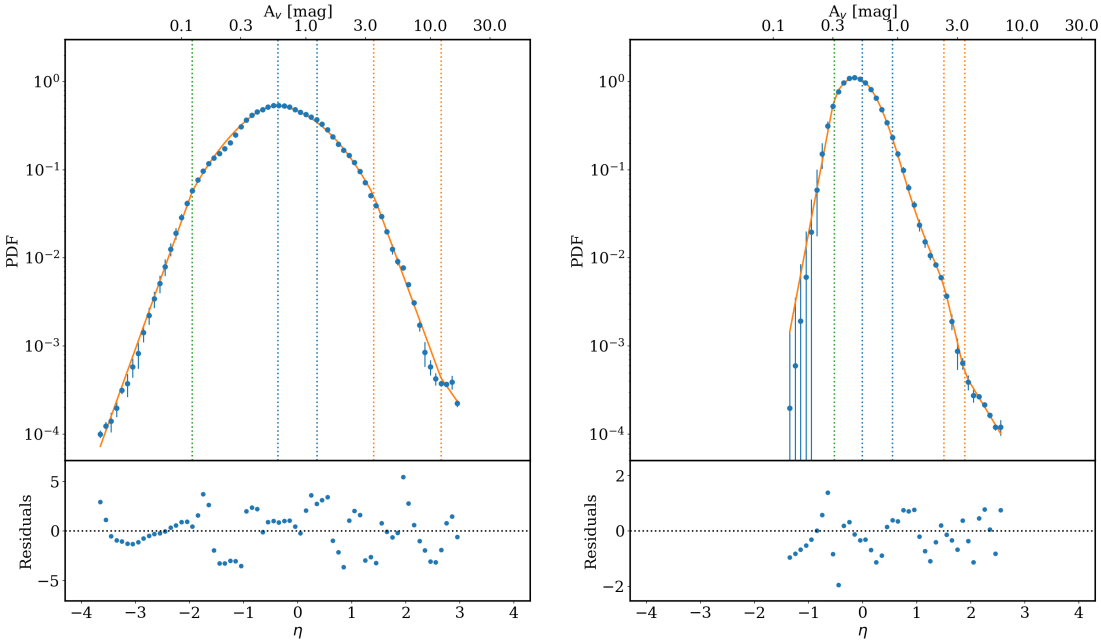

Fig. D.13: Cham III (left) and Polaris (right).

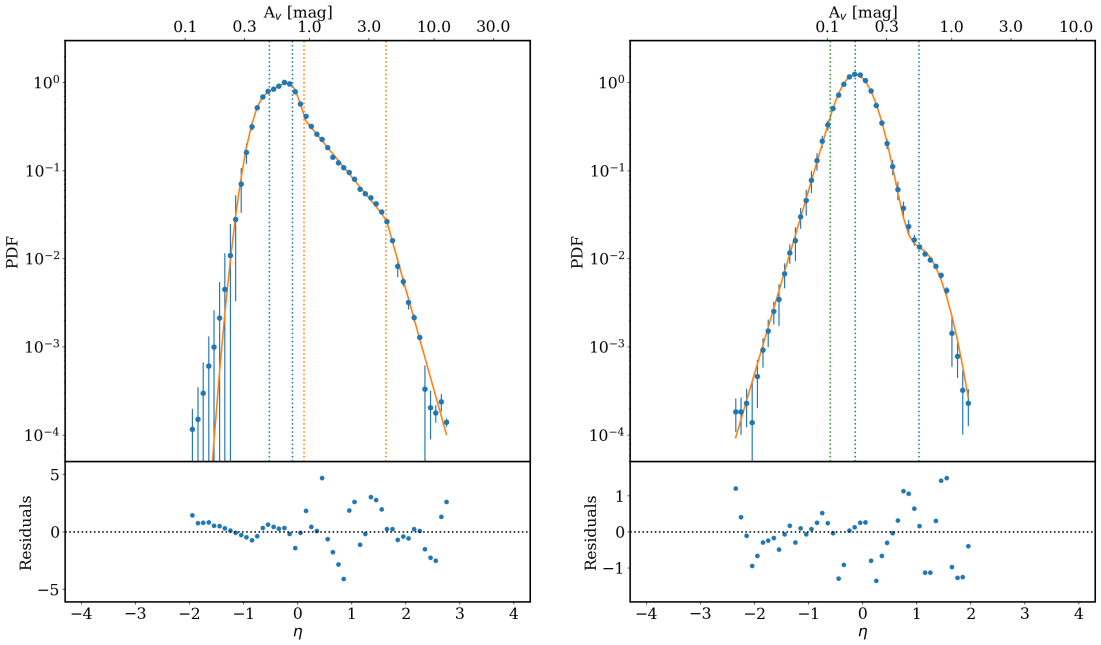

Fig. D.14: Musca (left) and Draco (right).

Appendix E: Correlations of N-PDF parameters with cloud type

Figures E.1, E.2 and E.3 display various N-PDF parameters and the exponents β_1 and β_2 determined using the Δ-variance given in Table 3 as a function of cloud mass as a proxy for cloud type. With these correlation plots, we explore possible systematic trends or thresholds.

Overall, we observe that the peak(s) of the N-PDF, A_V(peak1) and A_V(peak2), and the first and second deviation point, A_V(DP1) and A_V(DP2), increase with mass while all other parameters, the N-PDF width (σ), PLT slopes (s_1 and s_2) and β_1 and β_2 are rather independent of cloud type.

In Paper I, we fitted a single log-normal distribution at low column densities and derived that A_V(peak) increases with cloud mass. Here, we mostly fit two lognormals. The first peak for quiescent and low-mass regions is always below $A_V \sim 1$ while the second peak varies between $A_V \sim 0.5$ and 2. Both parameters show no dependence on mass, which would be consistent with our interpretation that the first log-normal is mostly constituted by atomic gas. For intermediate- and high-mass regions, the A_V for the first and second peak are overall higher, but there is no trend of an increase with mass. This would support the proposal that for high-mass and intermediate-mass regions, the second peak of the N-PDF can be attributed to a compressed layer of dense gas due to stellar feedback. The (column)-density of this layer depends on various factors such as external pressure, initial density etc. and can thus vary from cloud to cloud.

The widths of the log-normal parts of the N-PDF show no clear trends. There is a tendancy that quiescent and low-mass regions have smaller $\sigma_{\eta 1}$ (median values of 0.38 and 0.32 with respect to intermediate and high mass regions with $\sigma_{\eta 1}$ = 0.47 and 0.52, respectively). The width of the second log-normal is generally larger, median values for all cloud types range betweem 0.52 and 0.64.

The A_V value where the log-normal fit to the low column density part of the N-PDF crosses the observed N-PDF and the first PLT starts is defined as the first deviation point, A_V(DP1). Ignoring the A_V(DP1) numbers for the most massive clouds (black triangles in Fig. E.1), we find that the values cover a rather narrow range between A_V(DP1) $\sim$ 1 and A_V(DP1) $\sim$ 5 with a clustering around A_V(DP1) $\sim$ 2–5. These values are similar to those obtained by Kainulainen et al. (2011) using extinction maps, but slightly lower than the value of $A_V = 6.0 \pm 1.5$ of Froebrich & Rowles (2010), also derived from extinction maps, and those of Paper I with $A_V = 4.7 \pm 0.4$. To determine A_V(DP1) for massive clouds is delicate because if a second log-normal (or a "bump" in the N-PDF) occurs due to compression, it may hide an underlying PLT. In other words, the transition from a turbulence-dominated regime (log-normal N-PDF) into a gravity-dominated one (PLT) may occur at values around A_V.

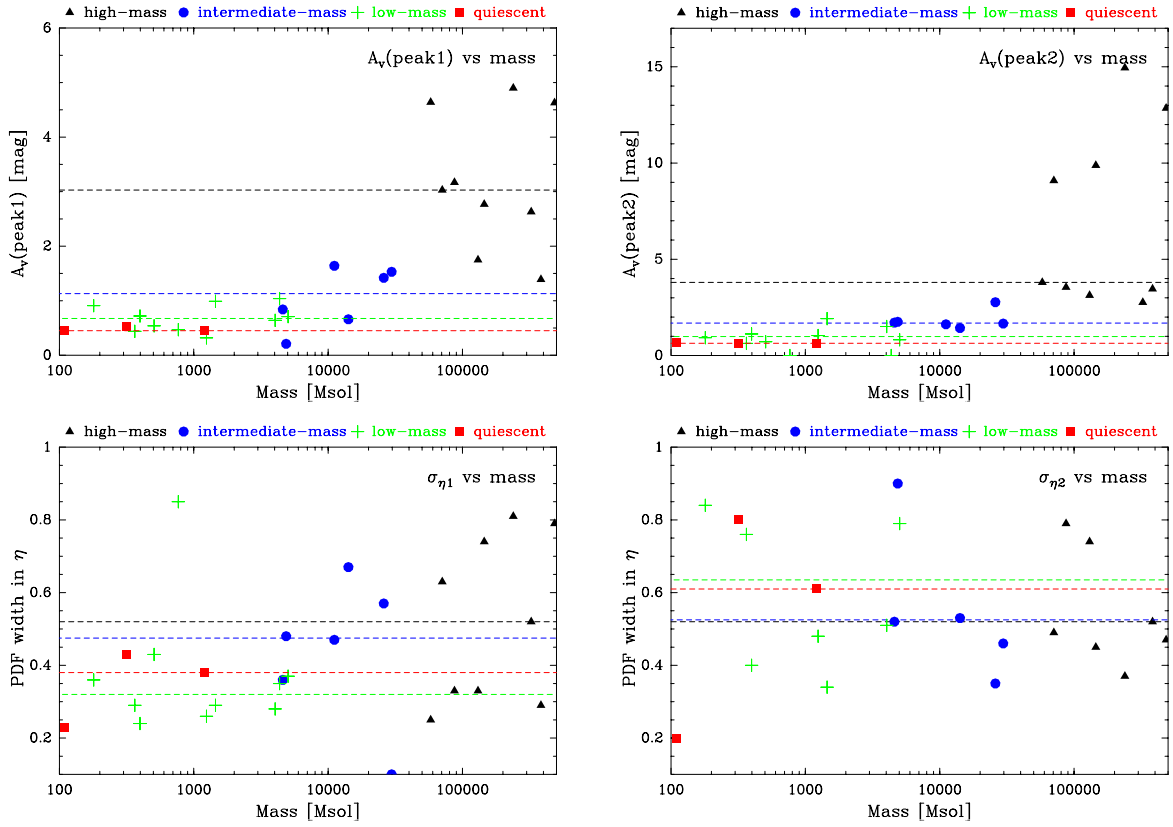

Fig. E.1: Correlation plots of N-PDF parameters as a function of mass as a proxy for the cloud type. The different cloud types are indicated with different colors and symbols. The median value for each cloud type is given in the respective color as a dashed line.

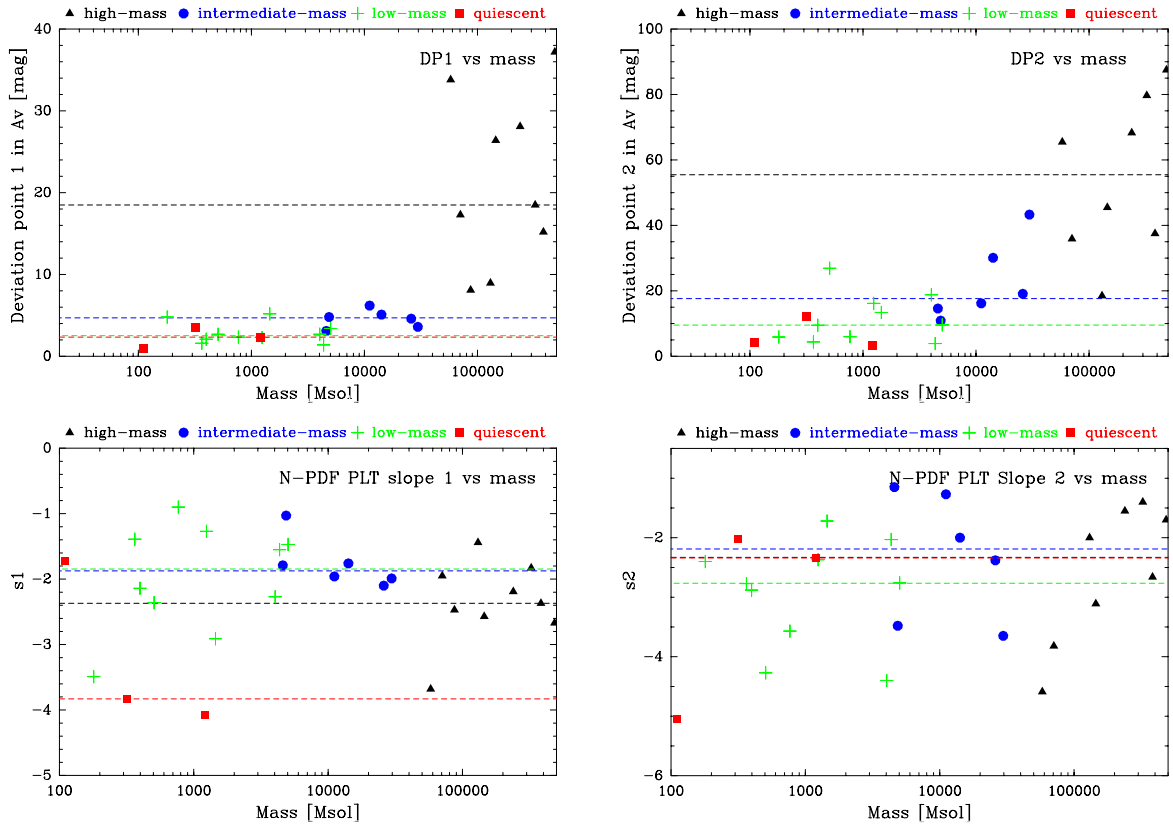

Fig. E.2: Correlation plots of N-PDF parameters as a function of mass as a proxy for the cloud type. The different cloud types are indicated with different colors and symbols. The median value for each cloud type is given in the respective color as a dashed line.

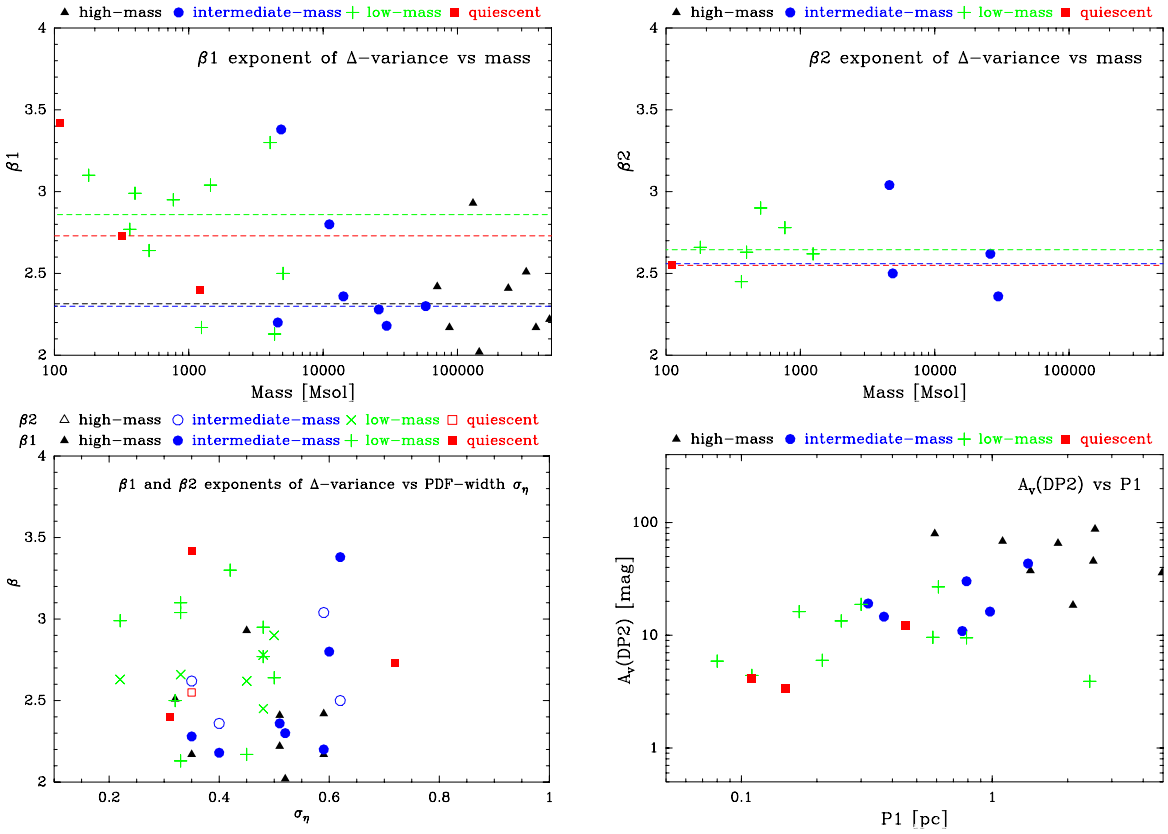

Fig. E.3: Correlation plots of β_1 and β_2 as a function of mass (top) as a proxy for the cloud type. The different cloud types are indicated with different colors and symbols. The median value for each cloud type is given in the respective color as a dashed line. The left bottom panel shows β_1 and β_2 against the width of the log-normal part of the N-PDF. The right bottom panel displays A_V(DP2) against P1 and indicates the A_V value where the slope change between first and second PLT in the N-PDF occurs, and the first characteristic size scale detected by the Δ-variance.